About the magnitude of the $\gamma^* N \to N(1520)$ transverse amplitudes near $Q^2 = 0$

G. Ramalho

Department of Physics and OMEG Institute, Soongsil University, Seoul 06978, Republic of Korea

(Received 27 December 2023; accepted 27 March 2024; published 16 April 2024)

The $\gamma^* N \to N(1520)$ transition has a property that differs from the other low-lying nucleon resonance amplitudes: the magnitude of the transverse helicity amplitudes. The transition helicity amplitudes are defined in terms of square-transfer momentum q^2, or $Q^2 = -q^2$. Near the photon point ($Q^2 = 0$) there is a significant difference in the magnitude of the transverse amplitudes: $A_{3/2}$ is very large and $A_{1/2}$ is very small. This atypical behavior contrasts with the relation between the amplitudes at the pseudothreshold [the limit where the nucleon and the $N(1520)$ are both at rest and $Q^2 < 0$], where $A_{3/2} = A_{1/2}/\sqrt{3}$, and also in the large-$Q^2$ region, where theory and data suggest that $A_{3/2}$ is suppressed relative to $A_{1/2}$. In the present work, we look for the source of the suppression of the $A_{1/2}$ amplitude at $Q^2 = 0$. The result is easy to understand in first approximation, when we look into the relation between the transverse amplitudes and the elementary form factors, defined by a gauge-invariant parametrization of the $\gamma^* N \to N(1520)$ transition current, near $Q^2 = 0$. There is a partial cancellation between contributions of two elementary form factors near $Q^2 = 0$. We conclude, however, that the correlation between the two elementary form factors at $Q^2 = 0$ is not sufficient to explain the transverse amplitude data below $Q^2 = 1$ GeV^2. The description of the dependence of the transverse amplitudes on Q^2 requires the determination of the scale of variation of the elementary form factors in the range $Q^2 = 0 \ldots 0.5$ GeV^2, a region with almost nonexistent data. We conclude at the end that the low-Q^2 data for the transverse amplitudes can be well described when we relate the scale of variation of the elementary form factors with the nucleon dipole form factor.

DOI: 10.1103/PhysRevD.109.074021

I. INTRODUCTION

In the last two decades there was a significant progress in the experimental study of the electromagnetic structure of the nucleon (N) and the nucleon resonances (N^*). The helicity amplitudes associated with the $\gamma^* N \to N^*$ transitions have been measured in detail for the $\Delta(1232)$, $N(1440)$, $N(1520)$, and $N(1535)$ resonances in a range from $Q^2 = 0.25$ GeV^2 up to 4 or 6 GeV^2 [1–6]. The measured helicity amplitudes are the transverse amplitudes $A_{1/2}$ and $A_{3/2}$ (for spin $J \geq 3/2$) and the longitudinal amplitude $S_{1/2}$. Near the photon point, however, there are still some uncertainties associated with the shape associated with the helicity amplitudes [1,7,8]. The selection from the Particle Data Group (PDG) at $Q^2 = 0$ has a large band of variation [9], and for most resonances there are no data below $Q^2 = 0.25$ GeV^2 [1,10].

Among the best known experimental resonances the $N(1520)\frac{3}{2}^-$ (spin $J = \frac{3}{2}$ and negative parity, $P = -$) has properties that differ from the other low-lying nucleon excitations. The transverse amplitudes $A_{1/2}$ and $A_{3/2}$ have completely different magnitudes near the photon point [9], and the helicity amplitudes are related by two conditions near the pseudothreshold point, where $Q^2 = -(M_R - M)^2$ [1,11] (M is the mass of the nucleon and M_R is the mass of the nucleon resonance). Most transitions are constrained by only one condition [1,7,11]. Although these constraints are valid in a region not directly accessed by electron scattering on nucleons ($Q^2 < 0$) that may not be probed directly in physical experiments, the relations may have a significant impact on the shape of the helicity amplitudes at low Q^2, when the masses of the nucleon and the nucleon resonance are close [1,7,8,12–14]. Numerically, the pseudothreshold occurs when $Q^2 \simeq -0.38$ GeV^2.

In the present work, we study the magnitude of the $\gamma^* N \to N(1520)$ transverse amplitudes near $Q^2 = 0$, based on the analytic structure of the transition current and on the correlations between the amplitudes in the low-Q^2 region. We start by reviewing what we know about the transverse amplitudes in three kinematic regions.

Near the pseudothreshold, in addition to the condition associated with Siegert's theorem [8,15–17], one has the relation $A_{3/2} = \sqrt{3}A_{1/2}$ [1,7,11]. In the large-Q^2 region, theoretical calculations based on constituent quark-counting rules and perturbative QCD arguments indicate that there is a strong dominance of the $A_{1/2}$ amplitude over the $A_{3/2}$ amplitude ($|A_{1/2}| \gg |A_{3/2}|$) [1,2,5,18]. Finally, near $Q^2 = 0$, one can quote the information from the PDG [9]:

$$\begin{aligned} A_{3/2} &= +(140 \pm 5) \times 10^{-3}\ \text{GeV}^{-1/2}, \\ A_{1/2} &= -(22.5 \pm 7.5) \times 10^{-3}\ \text{GeV}^{-1/2}. \end{aligned} \tag{1.1}$$

From these results, we can conclude that there is a considerable suppression of $A_{1/2}$ relative to $A_{3/2}$ at the photon point.

We can summarize our knowledge of the ratio $A_{1/2}/A_{3/2}$, in the three regimes, as

$$\mathcal{R} \equiv \frac{A_{1/2}}{A_{3/2}} = \begin{cases} \frac{1}{\sqrt{3}} & \text{if } Q^2 = -(M_R - M)^2 \\ -\epsilon & \text{if } Q^2 = 0 \\ \infty & \text{if } Q^2 = +\infty \end{cases}, \tag{1.2}$$

where ϵ represents a small positive value, $\epsilon \simeq 0.18 \simeq \frac{1}{5}$, according to the experimental data (1.1).

At the pseudothreshold, the amplitudes have similar magnitudes ($\mathcal{R} \simeq 0.6$). The suppression of $A_{3/2}$ at large Q^2 is extensively discussed in the literature [1,2,18,19]. The theoretical challenge is then to understand why the ratio between the two amplitudes is so small in absolute value near $Q^2 = 0$.

From the theoretical point of view, there is some debate about the nature of the $N(1520)$ resonance: if it is dominated by valence quark degrees of freedom, or alternatively, if it is dominated by baryon-meson molecular-like states [1,6,19,20]. The magnitude of $A_{3/2}(0)$ is difficult to explain based solely on the quark core structure of the baryon states. Quark model calculations explain in general only about one-third or one-half of the measured value of the amplitude [18,21–24]. Those estimates are improved when explicit meson cloud dressing or quark-antiquarks excitations are taken into account in quark model calculations [24,25]. Calculations based on dynamical coupled-channel reaction models, where the baryon resonances are described in terms of baryon-meson states [6,26,27], predict large contributions to the amplitude $A_{3/2}$ at low Q^2, on the order of 50% of the experimental values [20]. In the present work, we look for the origin of the difference of magnitudes between $A_{1/2}$ and $A_{3/2}$, based on the numerical contributions for each amplitude, without an explicit reference to the internal degrees of freedom.

The transverse amplitudes can be expressed in terms of the multipole form factors: the magnetic dipole (G_M) and the electric quadrupole (G_E) form factors, as defined by Devenish *et al.* [1,2,11],

$$A_{1/2} = -\frac{1}{4F}T_1, \qquad A_{3/2} = -\frac{\sqrt{3}}{4F}T_2, \tag{1.3}$$

where

$$T_1 \equiv G_E - 3G_M, \qquad T_2 \equiv G_E + G_M, \tag{1.4}$$

and the factor F takes the form

$$F = \frac{1}{e}\frac{2M}{M_R - M}\sqrt{\frac{MM_RK}{(M_R + M)^2 + Q^2}}, \tag{1.5}$$

with $K = \frac{M_R^2 - M^2}{2M_R}$, $e = \sqrt{4\pi\alpha}$, and $\alpha \simeq 1/137$ is the hyperfine structure constant.

From the previous relations, we can conclude that $A_{1/2} \simeq 0$, near $Q^2 = 0$ is equivalent to the result $G_E \simeq 3G_M$. Notice, however, that this analysis only transfers the discussion from helicity amplitudes to the multipole form factors G_E and G_M, and tells us nothing about the correlation between G_E and G_M.

The results $A_{1/2} \simeq 0$ or $G_E \simeq 3G_M$ can be understood when we write the relations between the helicity amplitudes and the multipole form factors in terms of the elementary form factors, defined by the gauge-invariant representation of the transition current for a $J^P = \frac{3}{2}^-$ nucleon resonance. The transition current can be expressed in terms of three independent gauge-invariant structures which define three independent forms factors that can be labeled as G_1, G_2, and G_3, and are free of kinematic singularities [1,11]. For convenience, we call these functions elementary form factors.

Using the elementary form factors, we can rewrite the transverse amplitudes (1.3) in the limit $Q^2 = 0$, as

$$A_{1/2} = -\frac{1}{4F_0}T_1, \tag{1.6}$$

$$A_{3/2} = -\frac{\sqrt{3}}{4F_0}\left[T_1 - 4\frac{M}{\sqrt{6}}\frac{M_R - M}{M_R}G_1\right], \tag{1.7}$$

where $F_0 = \mathcal{B}\sqrt{M}$ and $\mathcal{B} = \frac{1}{e}\frac{M}{M_R}\sqrt{\frac{M_R}{K}} \simeq 3.67$ is dimensionless. The factor T_1, defined by Eqs. (1.4), takes the form

$$T_1 = -4\frac{M}{\sqrt{6}}\left[\frac{M}{M_R}G_1 + \frac{1}{2}(M_R + M)G_2\right]. \tag{1.8}$$

From the relations (1.6)–(1.8), we can then conclude that in the limit $Q^2 = 0$, the transverse amplitudes depend only on the values of the functions G_1 and G_2. We can also conclude that $A_{1/2} \simeq 0$, when T_1 is negligible, and as a

consequence $A_{3/2} \propto \frac{M_R - M}{M_R} G_1$ is large when G_1 is large. The numerical result for $A_{1/2}$ is then explained when G_1 and G_2 are large and have opposite signs. In this case, there is a significant cancellation between the terms in G_1 and in G_2. We will conclude, however, that $T_1 \simeq 0$ ($\epsilon \simeq 0$) provide only a rough explanation of the data. The values of G_1 and G_2 at $Q^2 = 0$ have corrections of the order of 30 and 20%, respectively, when we use the experimental ratio $A_{1/2}/A_{3/2}$ ($\epsilon \simeq 0.2$), instead of $A_{1/2} = 0$ ($\epsilon = 0$).

At this point, one can ask if the values of $G_1(0)$ and $G_2(0)$ can help to explain the Q^2 dependence of $A_{1/2}$ and $A_{3/2}$ in the range $Q^2 = 0 \ldots 1$ GeV^2. A simple numerical calculation demonstrates, however, that the shape of the amplitude $A_{3/2}$ cannot be explained without an estimate of the derivative of the elementary form factors G_i. We conclude at the end that the $A_{1/2}$ and $A_{3/2}$ data can be well described when we consider simple multipole parametrizations of the form factors G_i, where the scale of variation is determined by the scale of the nucleon dipole form factor, used in parametrizations of the nucleon electromagnetic form factors and some $\gamma^* N \to N^*$ transition form factors.

We propose parametrizations of the $A_{1/2}$ and $A_{3/2}$ amplitudes based on our analysis of the amplitudes at $Q^2 = 0$. The parametrizations are consistent with the $Q^2 = 0 \ldots 1$ GeV^2 data, within the uncertainties of the available data, and may be tested by future experiments in facilities like MAMI or JLab-12 GeV in the low-Q^2 region [10]. The precision of the present estimates can be improved once the uncertainties of the $A_{1/2}(0)$ and $A_{3/2}(0)$ data are reduced.

This article is organized as follows: in the next section we present the general formalism for the $\gamma^* N \to N^*$ transition form factors and helicity amplitudes for $J^P = \frac{3}{2}^-$ nucleon resonances, and discuss the relevant limits (pseudothreshold, photon point, and large Q^2). Our numerical analysis of the elementary form factors at the photon point is presented in Sec. III. In Sec. IV, we derive parametrizations of the data based on the our analysis and discuss the limits of the parametrizations. We finalize in Sec. IV with the outlook and conclusions.

II. HELICITY AMPLITUDES AND TRANSITION FORM FACTORS

We discuss now the formalism associated with the $\gamma^* N \to N(1520)$ transition, and the definition of helicity amplitudes and multipole form factors.

Considering an initial nucleon with the momentum p and a final nucleon resonance with momentum p', we can define

$$q = p' - p, \qquad P = \frac{1}{2}(p' + p), \tag{2.1}$$

as the transfer momentum and the average of the baryons momentum, respectively.

The transition current between a nucleon and an N^* $J^P = \frac{3}{2}^-$ state can be written as

$$J^\mu = \bar{u}_\alpha(p') \Gamma^{\alpha\mu}(P, q) \gamma_5 u(p), \tag{2.2}$$

where u_α, u are the resonance and the nucleon spinors, respectively, and $\Gamma^{\alpha\mu}$ takes the form [1,2,11,19,28]

$$\Gamma^{\alpha\mu}(P, q) = \left(q^\alpha \gamma^\mu - \not{q} g^{\alpha\mu}\right) G_1 + \left[q^\alpha P^\mu - (P \cdot q) g^{\alpha\mu}\right] G_2 + \left(q^\alpha q^\mu - q^2 g^{\alpha\mu}\right) G_3. \tag{2.3}$$

In the previous relation, G_i ($i = 1, 2, 3$) are independent functions, free of kinematic singularities, referred to hereafter as elementary form factors. Comparatively with other authors that use the Devenish convention for the operators, and define the second term of Eq. (2.3) in terms of $p' = P + \frac{1}{2} q$ [1,2,11], we follow the Jones and Scadron convention [29] and use P to define the operator associated with G_2 [12,19,28,29]. The conversion is trivial.[1]

For the representation of the helicity amplitudes, defined at the resonance rest frame, it is convenient to introduce the magnitude of the transfer three-momentum $|\mathbf{q}|$. This variable can be written in a covariant form as

$$|\mathbf{q}| = \frac{\sqrt{Q_+^2 Q_-^2}}{2M_R}, \tag{2.4}$$

using the notation

$$Q_\pm^2 = (M_R \pm M)^2 + Q^2. \tag{2.5}$$

The magnetic dipole (G_M) and the electric quadrupole (G_E) form factors can be calculated inverting the relations (1.3) and (1.4):

$$G_M = -F\left[\frac{1}{\sqrt{3}} A_{3/2} - A_{1/2}\right], \tag{2.6}$$

$$G_E = -F\left[\sqrt{3} A_{3/2} + A_{1/2}\right]. \tag{2.7}$$

One can also relate the longitudinal (scalar) amplitude $S_{1/2}$ with the Coulomb quadrupole form factor G_C,

$$S_{1/2} = -\frac{1}{\sqrt{2}F} \frac{|\mathbf{q}|}{2M_R} G_C. \tag{2.8}$$

Using the expressions (2.2) and (2.3), we can write the magnetic dipole and the electric quadrupole form factors in terms of G_i, as [1,2]

[1]To obtain the Devenish form factors [11] in terms of the Jones and Scadron form factors [29] we replace $G_1 \to G_1$, $G_2 \to G_2$, and $G_3 \to G_3 + \frac{1}{2} G_2$.

$$G_M = -Z_R Q_-^2 \frac{G_1}{M_R}, \tag{2.9}$$

$$G_E = -Z_R \Big\{ \big[(3M_R + M)(M_R - M) - Q^2\big] \frac{G_1}{M_R} + 2\big(M_R^2 - M^2\big) G_2 - 4Q^2 G_3 \Big\}, \tag{2.10}$$

where $Z_R = \frac{1}{\sqrt{6}} \frac{M}{M_R - M}$.

Using the previous equations, we conclude that

$$T_1 = -Z_R \Big\{ 4\big[M(M_R - M) - Q^2\big] \frac{G_1}{M_R} + 2\big(M_R^2 - M^2\big) G_2 - 4Q^2 G_3 \Big\}, \tag{2.11}$$

$$T_2 = -Z_R \big\{ 4(M_R - M) G_1 + 2\big(M_R^2 - M^2\big) G_2 - 4Q^2 G_3 \big\}. \tag{2.12}$$

We can also write

$$T_2 = T_1 - 4 Z_R Q_-^2 \frac{G_1}{M_R} = T_1 + 4 G_M. \tag{2.13}$$

For future discussion, we write also the relation between the Coulomb quadrupole form factor and the elementary form factors,

$$G_C = Z_R \big[4 M_R G_1 + (3M_R^2 + M^2 + Q^2) G_2 + 2(M_R^2 - M^2 - Q^2) G_3 \big]. \tag{2.14}$$

The previous relation can be used to calculate the amplitude $S_{1/2}$, according to Eq. (2.8). Notice that $S_{1/2}$ and G_C cannot be measured at the photon point (because there are no real photons with zero polarization). The relation (2.14) can be used, however, to estimate G_C and G_3 for values of Q^2 arbitrarily close to $Q^2 = 0$.

We discuss now briefly the three relevant limits: the pseudothreshold, the photon point, and the large-Q^2 limit.

A. Pseudothreshold

As mentioned already, when we study the electromagnetic properties based on the helicity amplitudes or the multipole form factors, there are some conditions between those functions that need to be fulfilled when we consider the pseudothreshold limit $Q^2 = -(M_R - M)^2$ [1,11]. These conditions are the consequence of the gauge-invariance structure of the transition current, which requires that the elementary form factors are independent and free of kinematic singularities [11,29].

There are two conditions to be considered for the $\gamma^* N \to N(\frac{3}{2}^-)$ multipole transition form factors [11,12]:

$$G_M \propto |\mathbf{q}|^2, \qquad G_C = -\frac{M_R - M}{M_R} G_E. \tag{2.15}$$

These conditions can be transposed to the helicity amplitudes, as [7,8]

$$A_{3/2} = \sqrt{3} A_{1/2}, \tag{2.16}$$

$$\big(A_{1/2} + \sqrt{3} A_{3/2}\big) = -2\sqrt{2}(M_R - M) \frac{S_{1/2}}{|\mathbf{q}|}. \tag{2.17}$$

In addition, it is expected that $S_{1/2} \propto \mathcal{O}(|\mathbf{q}|)$ and $A_{1/2}$, $A_{3/2} \propto \mathcal{O}(1)$, near $|\mathbf{q}| = 0$ [7,16].

The correlation between the transverse amplitudes (2.16) is equivalent to the relation $G_M = 0$ from (2.15) when $|\mathbf{q}| = 0$.

The second condition for the helicity amplitudes relates the electric amplitude, $E \equiv (A_{3/2} + \sqrt{3} A_{1/2})$, with the scalar amplitude $S_{1/2}$, and correspond to Siegert's theorem for the $J^P = \frac{3}{2}^-$ nucleon resonances [1,8,14,16,17,30–32].

Using the relations between the helicity amplitudes and the multipole form factors (2.9) and (2.10), and $G_M = 0$, we can conclude that

$$A_{3/2} = \sqrt{3} A_{1/2} = -\frac{\sqrt{3}}{4F} G_E, \tag{2.18}$$

where $F = \frac{1}{e} \frac{M}{\sqrt{2} M_R} \sqrt{\frac{M_R + M}{M_R - M}}$.

The conditions (2.15) for the form factors are valid for the nucleon resonances $J^P = \frac{3}{2}^-, \frac{5}{2}^+, \frac{7}{2}^-, \ldots$. Modified versions of the conditions for the helicity amplitudes (2.16) and (2.17) are also valid for $J^P = \frac{5}{2}^+, \frac{7}{2}^-, \ldots$ [1]. Among all those nucleon resonances, the $N(1520)\frac{3}{2}^-$ resonance is one of the resonances with stronger impact of the pseudothreshold conditions on parametrizations compatible with the available data [7], due to the proximity between pseudothreshold and photon points.

B. Photon point

In the limit $Q^2 = 0$, we can write

$$T_1 = -4 \frac{M}{\sqrt{6}} \Big\{ \frac{M}{M_R} G_1 + \frac{1}{2}(M_R + M) G_2 \Big\}, \tag{2.19}$$

$$T_2 = -4 \frac{M}{\sqrt{6}} \Big\{ G_1 + \frac{1}{2}(M_R + M) G_2 \Big\}. \tag{2.20}$$

We can also write, following Eq. (2.13),

$$T_2 = T_1 - 4\frac{M}{\sqrt{6}}(M_R - M)\frac{G_1}{M_R} = T_1 + 4G_M, \tag{2.21}$$

and

$$G_M = -\frac{M}{\sqrt{6}}(M_R - M)\frac{G_1}{M_R}. \tag{2.22}$$

To obtain the previous relations, we used $(M_R - M)Z_R = \frac{M}{\sqrt{6}}$.

Concerning the scalar amplitude, we can write

$$F_0 S_{1/2}(0) = -\frac{1}{2\sqrt{3}}\frac{M(M_R+M)}{4M_R^2} \times \left[4M_R G_1 + \left(3M_R^2 + M^2\right)G_2 + 2\left(M_R^2 - M^2\right)G_3\right]. \tag{2.23}$$

C. Large Q^2

The large-Q^2 region has been discussed in detail in the literature [1,2]. Here, we present the summary. At large Q^2 the transverse amplitudes follow [1,33,34]

$$A_{1/2} \propto \frac{1}{Q^3}, \qquad A_{3/2} \propto \frac{1}{Q^5}, \tag{2.24}$$

meaning that $A_{3/2}$ is suppressed relatively to $A_{1/2}$.

The corresponding relations for the form factors are [1,19]

$$G_E \propto \frac{1}{Q^4}, \qquad G_M \propto \frac{1}{Q^4}, \tag{2.25}$$

$$G_E = -G_M + \mathcal{O}\left(\frac{1}{Q^6}\right). \tag{2.26}$$

III. FORM FACTORS G_i FOR $Q^2 = 0$

In the analysis of the transverse amplitudes near $Q^2 = 0$, we consider different approximations. For the discussion, we convert the experimental data (1.1), into the dimensionless variables

$$\tilde{A}_{3/2} = F_0 A_{3/2}(0) = +0.498 \pm 0.018, \tag{3.1}$$

$$\tilde{A}_{1/2} = F_0 A_{1/2}(0) = -0.080 \pm 0.027, \tag{3.2}$$

based on the numerical result $F_0 = 3.67\sqrt{M}$.

Notice that since the comparison between amplitudes is made in units $10^{-3}\,\mathrm{GeV}^{-1/2}$, the first quantity ($\simeq 500 \times 10^{-3}$) can be regarded as a large number, and the second quantity ($\simeq -80 \times 10^{-3}$) can be regarded as a small number.

We can use the results (3.1) and (3.2), to calculate the corresponding form factors G_1 and G_2 for $Q^2 = 0$. Inverting the relations (1.6)–(1.8), one obtains

$$MG_1 = \mathcal{R}\left(\frac{1}{\sqrt{3}}\tilde{A}_{3/2} - \tilde{A}_{1/2}\right), \tag{3.3}$$

$$M^2 G_2 = -\frac{2M}{M_R + M}\frac{M}{M_R}\mathcal{R}\left(\frac{1}{\sqrt{3}}\tilde{A}_{3/2} - \frac{M_R}{M}\tilde{A}_{1/2}\right), \tag{3.4}$$

where $\mathcal{R} = \frac{\sqrt{6}M_R}{M_R - M}$. The factors M and M^2 are included to generate dimensionless expressions.

In the Introduction, we discussed the approximation $\tilde{A}_{1/2} = 0$ ($T_1 = 0$), based on Eqs. (1.6) and (1.7). In that case, we obtain $G_2 = -\frac{2}{M_R+M}\frac{M}{M_R}G_1$. Now, we can notice, using the relations (3.3) and (3.4), that the condition $T_1 = 0$ provides only a rough approximation, since $\tilde{A}_{1/2}$ is combined in fact with $\tilde{A}_{3/2}/\sqrt{3}$. Neglecting $\tilde{A}_{1/2}$ in the estimates of G_1 and G_2 has an impact of 28% for G_1 and of 17% for G_2.

The relations (3.3) and (3.4) can also be used to explain the significant cancellation in T_1. The effect can be observed when we write T_1 on the form $T_1 = -4\frac{M}{\sqrt{6}}t_1$, where

$$t_1 = \frac{M}{M_R}G_1 + \frac{1}{2}(M_R + M)G_2. \tag{3.5}$$

For that purpose, we write the two terms as

$$\frac{M}{M_R}G_1 = \frac{\mathcal{R}}{M_R}\left(\frac{1}{\sqrt{3}}\tilde{A}_{3/2} - \tilde{A}_{1/2}\right),$$
$$\frac{1}{2}(M_R + M)G_2 = -\frac{\mathcal{R}}{M_R}\left(\frac{1}{\sqrt{3}}\tilde{A}_{3/2} - \tilde{A}_{1/2}\right) + \frac{\mathcal{R}}{M_R}\frac{M_R - M}{M}\tilde{A}_{1/2}.$$

In this form, one concludes that the first term of $\frac{1}{2}(M_R + M)G_2$ cancels the term in G_1, and only the term proportional to $\tilde{A}_{1/2}$ survives the sum. The correction term is 13% of the term in G_1. In units 10^{-3} the term in G_1 and the term in G_2 are large numbers with opposite signs.

The dominance of the amplitude $A_{3/2}$ is still explained by the small magnitude of T_1. When we can neglect T_1 in Eq. (2.21), we conclude that $T_2 \propto G_1$. Thus, the amplitude $A_{3/2}$ is large when T_2 is large, and T_1 is small in comparison with T_2. However, when we look for (2.20): $T_2 = -4\frac{M}{\sqrt{6}}t_2$, with $t_2 = G_1 + \frac{1}{2}(M_R + M)G_2$, we conclude that T_2 is large because there is only a partial cancellation between the two large terms.

To summarize, the combination of the results for the transverse amplitudes is a consequence of the large

TABLE I. Model parameters $G_1(0)$, $G_2(0)$, according with the values for the amplitudes $A_{3/2}(0)$, $A_{1/2}(0)$. We include also the limit of $S_{1/2}(Q^2)$ for $Q^2 = 0$, based on the values of $G_3(0)$. The amplitudes are in units 10^{-3} GeV$^{-1/2}$. In the last row, the values between commas are the uncertainties of $MG_1(0)$ and $M^2G_2(0)$, based on the data for the transverse amplitudes. The model with $T_1 \neq 0$ has $T_2 = -1.149$.

	$MG_1(0)$	$M^2G_2(0)$	$M^2G_3(0)$	$A_{3/2}(0)$	$A_{1/2}(0)$	$S_{1/2}(0)$	$G_M(0)$	$G_E(0)$	Label
$T_1 = 0$	2.507	−1.429		140	0.0		−0.287	−0.862	
$T_1 = 0.319$	2.354	−1.260	0.000	140	−22.5	−82.7	−0.367	−0.782	Multipole 2a
	2.354	−1.260	−0.140	140	−22.5	−73.5	−0.367	−0.782	Multipole 2b
	2.354	−1.260	−0.278	140	−22.5	−64.4	−0.367	−0.782	Multipole 2c
	(0.183)	(0.134)							

magnitude of the form factors G_1 and $-G_2$. In $A_{1/2}$, one has a significant cancellation between the term in G_1 and the term in G_2. In $A_{3/2}$, the term in G_1 is enhanced and the suppression between the terms is attenuated. We conclude also that in first approximation (leading order in $\tilde{A}_{1/2}$), one has $A_{3/2} \propto G_1$.

The values of G_1 and G_2 for $Q^2 = 0$ are presented in Table I for the cases $T_1 = 0$ and $T_1 \neq 0$. The first row ($T_1 = 0$) gives the results when we use $A_{1/2}(0) = 0$, and the second row gives the result when $T_1 \neq 0$ is fixed by the experimental value of $A_{1/2}(0)$. In the second row, we include also $G_3(0) = 0$. The last four rows and the effect of $G_3(0)$ are discussed in the next sections.

The comparison between the first two rows demonstrates how important the inclusion of the experimental value of $A_{1/2}(0)$, instead of $A_{1/2}(0) = 0$, is in the determination of the first two elementary form factors. The effect can also be seen in the results for $G_M(0)$ and $G_E(0)$. The differences are about 20% for the magnetic form factor and 10% for the electric form factor.

In the next sections, we use the estimated values for G_1 and G_2 at $Q^2 = 0$ to test if we can derive parametrizations that may explain the experimental data for the amplitudes $A_{1/2}$ and $A_{3/2}$, up to a certain range of Q^2. Due to the approximated character of the parametrizations, we restrict the analysis to the region $Q^2 < 1$ GeV^2. To estimate the uncertainties of the parametrizations, we calculate also the uncertainties of G_1 and G_2 at $Q^2 = 0$, based on the relations (3.3) and (3.4) and the data (1.1), with the errors combined in quadrature. The numerical values for the uncertainties of $G_1(0)$ and $G_2(0)$ are included in the last row of Table I (between brackets). The relative errors are 7.8% for G_1 and 10.6% for G_2.

IV. FORM FACTORS G_i FOR $Q^2 > 0$

In this section, we discuss possible parametrizations of the amplitudes $A_{1/2}$ and $A_{3/2}$ for $Q^2 \leq 1$ GeV^2 based on the values of $G_1(0)$ and $G_2(0)$ calculated in the previous section.

In the following, we consider the $\gamma^* N \to N(1520)$ helicity amplitude data from experiments at JLab/CLAS on single-pion electroproduction [35] and on charged double-pion electroproduction [20,36], and the PDG selection for $Q^2 = 0$ [9]. These JLab/CLAS experiments determine the whole set of helicity amplitudes ($A_{1/2}$, $A_{3/2}$, and $S_{1/2}$). The πN (∼60%) and the $\pi\pi N$ (∼30%) channels are the dominant $N(1520)$ decay channels [9]. There are additional data associated with different experiments for the transverse amplitudes [37], but the data analysis is based on the assumption that $S_{1/2} \equiv 0$, an approximation that is not valid at low Q^2 [35].

In a first stage, we ignore the role of the form factor G_3, setting $G_3 \equiv 0$, since no information about G_3 can be obtained from the transverse amplitudes at $Q^2 = 0$. We notice, however, that G_3 contributes to the amplitudes $A_{1/2}$ and $A_{3/2}$ for $Q^2 \neq 0$, since T_1 and T_2 include the term $4Z_R Q^2 G_3$ [see Eqs. (2.11) and (2.12)]. Later on, we estimate the impact of nonzero values for $G_3(0)$.

From the previous section, we concluded already that $A_{1/2}(0) \simeq 0$ is not a very good approximation. In the following, we consider then parametrizations based on Eqs. (3.3) and (3.4) consistent with the experimental value of $A_{1/2}(0)$. The numerical values are included in the lower part of Table I (with $T_1 = 0.319$).

We divided our analysis into several steps.

A. Parametrization with constant form factors G_i

The simplest parametrization can be obtained assuming that the form factors $G_1(Q^2)$ and $G_2(Q^2)$ do not vary significantly in the region $Q^2 = 0 \ldots 1$ GeV^2 (meaning that in that range the derivatives of those form factors are zero or negligible). We label this approximation as the constant form factor parametrization. The values of $G_i(0)$ are the ones presented on Table I in the first row with $T_1 = 0.319$. As mentioned already, we assume for now that $G_3(0) = 0$.

The constant form factor estimates are presented in Fig. 1 for the amplitudes and in Fig. 2 for the multipole form factors. Notice in the figures the lack of data for the interval

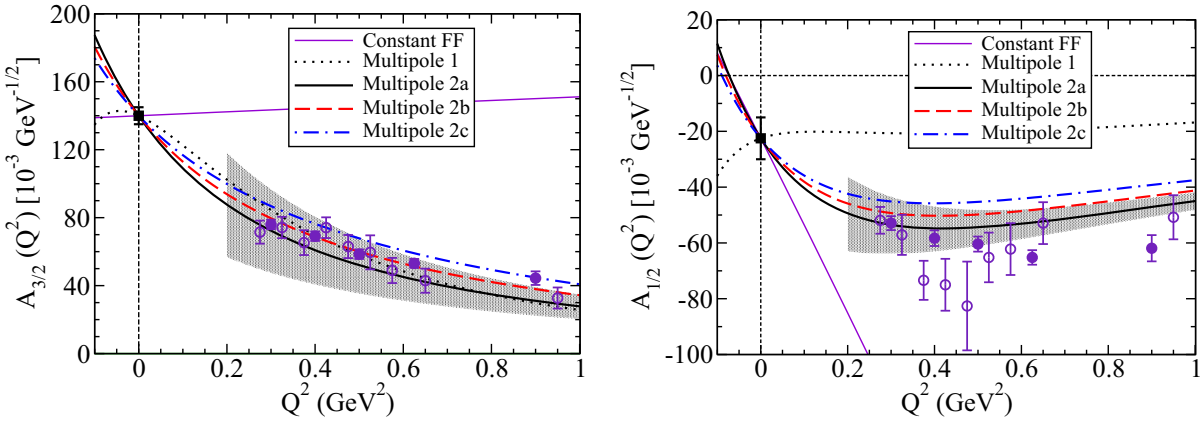

FIG. 1. Transverse amplitudes $A_{1/2}$ and $A_{3/2}$ in terms of Q^2. The data are from JLab/CLAS single-pion production (solid bullets) [35], JLab/CLAS double-pion production (empty bullets) [20,36], and PDG (square) [9]. The labels correspond to the parameters from Table I.

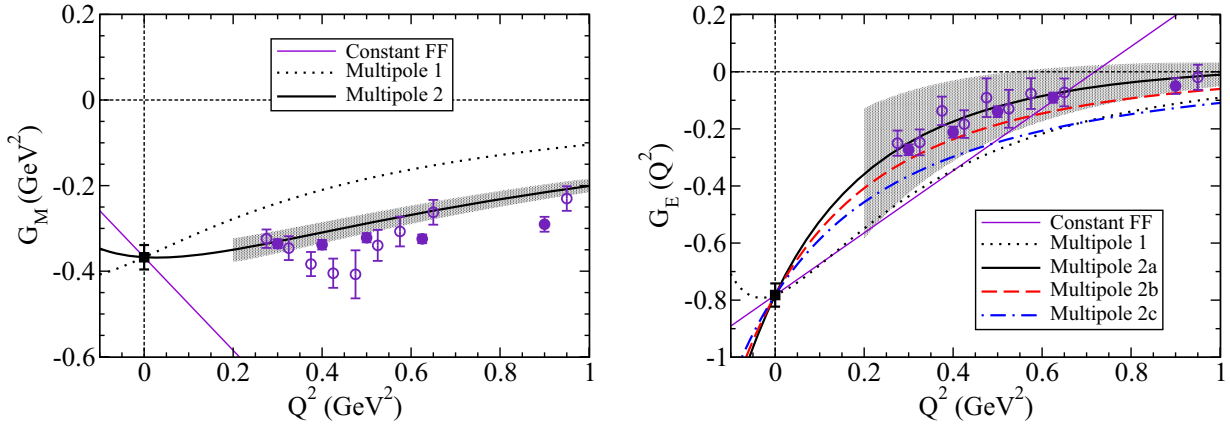

FIG. 2. Multipole form factors G_E and G_M in terms of Q^2. Data description as in Fig. 1. The labels correspond to the parameters from Table I.

$Q^2 = 0\ldots0.28$ GeV^2. This omission causes difficulty in the determination of the shape of the helicity amplitudes near the photon point [1,7].

In Figs. 1 and 2, we distinguish between the CLAS data from single-pion production [35] from double-pion production [20,36]. Some differences between the two sets can be observed for the function $A_{3/2}$ and G_M in the range $Q^2 = 0.35\ldots0.50$ GeV^2. The data are, however, compatible within the two standard deviation range. More accurate data in that range may help to determine the shape of the transverse amplitudes at low Q^2.

We present the calculations in the range $Q^2 = -0.1\ldots1$ GeV^2 for a better visualization of the results near $Q^2 = 0$. The lower limit of the graph in Q^2 can be extended down to the pseudothreshold $Q^2 \simeq -0.4$ GeV^2 in order to visualize the consequences of the pseudothreshold constraints. We notice, however, that the pseudothreshold conditions are automatically satisfied by the use of elementary form factors G_i when they have no singularities in the range $Q^2 > -(M_R - M)^2$. At the end, we discuss the properties of G_M near the pseudothreshold.

Before discussing the amplitudes $A_{1/2}$ and $A_{3/2}$ it is important to discuss the properties of the form factors G_E and G_M when the form factors G_i are constants. From the relations (2.9) and (2.10), we can conclude that the multipole form factors (G_E and G_M) are linear functions of Q^2.

As for the transverse amplitudes, we can notice that they are written in the form $A_{1/2} \propto \sqrt{1+\tau}T_1$ and $A_{3/2} \propto \sqrt{1+\tau}T_2$, where T_1 and T_2 are linear functions and $\tau = Q^2/(M_R + M)^2$ [see Eqs. (1.3)–(1.5)]. Since in the region of study $\tau \ll 1$ (because $Q^2 \ll 6.05$ GeV^2), one can write $\sqrt{1+\tau} \simeq 1 + \frac{1}{2}\frac{Q^2}{(M_R+M)^2}$, and conclude that in the region $Q^2 \leq 1$ GeV^2, the amplitudes are well approximated by linear functions.

We can now discuss the numerical results for the amplitudes $A_{1/2}$ and $A_{3/2}$ within the constant form factor approximation. The estimates are presented in Fig. 1 by the

thin solid line (labeled as Constant FF). The model estimate $A_{3/2} \simeq 140 \times 10^{-3}$ GeV$^{-1/2}$ contrasts with the sharp suppression of the experimental amplitude, when Q^2 increases. The estimate of $A_{3/2}$ manifests only a weak dependence on Q^2, because $A_{3/2} \propto \sqrt{1+\tau} T_2$ and T_2 is a constant. The conclusion is then that the amplitude $A_{3/2}$ follows $A_{3/2} \propto 1 + \frac{1}{2}\frac{Q^2}{(M_R+M)^2}$, in the range of study, an almost constant function. As for the amplitude $A_{1/2}$, we observe also an almost linear function[2] of Q^2, in flagrant disagreement with the data. The conclusion is then that the constant form factor approximation for the functions G_i fails completely the description of the amplitudes $A_{1/2}$ and $A_{3/2}$.

The corresponding results for G_E and G_M are presented in Fig. 2. In this case, one obtains linear functions, which fail in general the description of the data.

The corollary of this first analysis is that the description of the transverse amplitudes requires in addition to the values of the functions G_1 and G_2 at $Q^2 = 0$ the determination of the scale of variation of those functions. In simple terms, we need an estimate of the derivatives of the form factors G_1, G_2, and eventually G_3, if we want to describe the data in the range $Q^2 = 0 \ldots 1$ GeV^2.

B. Parametrization of G_i by multipole functions—universal cutoff

Once concluded that the data are not consistent with parametrizations based on constant elementary form factors, we look for parametrizations based on multipole functions. These kinds of parametrizations are considered, for instance, in the study of the nucleon electromagnetic form factors, where the main dependence is regulated by a simple dipole function. Based on the expected asymptotic dependence of the functions G_i in the large-Q^2 region, we consider the multipole parametrizations

$$G_1(Q^2) = \frac{G_1(0)}{\left(1+\frac{Q^2}{\Lambda_3^2}\right)^3}, \qquad G_{2,3}(Q^2) = \frac{G_{2,3}(0)}{\left(1+\frac{Q^2}{\Lambda_4^2}\right)^4}, \quad (4.1)$$

where we labeled the square form factor cutoffs Λ_n^2 by the power n of the multipole. We assume then that G_2 and G_3 [when $G_3(0) \neq 0$] are regulated by the same cutoff. The powers of Eq. (4.1) are the ones compatible with the expected falloffs for the helicity amplitudes (2.24) and the multipole form factors (2.25) and (2.26).

The multipole functions take into account implicitly the leading-order dependence of the form factors G_i on Q^2. The method had been used in chiral effective-field theory to include next-leading-order contributions and improve the convergence of the calculations [38]. It is also known that simple smooth parametrizations of $\gamma^* N \to N^*$ data are obtained for most low-lying nucleon resonances when the functions are normalized by an appropriated multipole [39].

One of the simplest parametrizations is obtained when we assume that the scale of variation of the form factors G_i (associated with the square cutoffs Λ_3^2 and Λ_4^2) can be the same for all the form factors ($\Lambda_3^2 = \Lambda_4^2$). The condition $\Lambda_3^2 = \Lambda_4^2$ defines the universal cutoff approximation.

Inspired by the nucleon dipole function

$$G_D(Q^2) = \frac{1}{\left(1+\frac{Q^2}{\Lambda_D^2}\right)^2}, \quad (4.2)$$

where $\Lambda_D^2 = 0.71$ GeV^2, we consider a parametrization where

$$\Lambda_3^2 = \Lambda_4^2 = \Lambda_D^2. \quad (4.3)$$

The results of the universal form factor parametrization are represented in Figs. 1 and 2 by the dotted line and are labeled as Multipole 1. We can notice in the figure for the amplitudes (Fig. 1) the failure in the description of the amplitude $A_{1/2}$. Also worth noticing is the shape of the amplitude $A_{3/2}$ near $Q^2 = 0$. Although no data exist below $Q^2 = 0.28$ GeV^2, theoretical models predict in general a sharp and fast falloff of the amplitude near $Q^2 = 0$. In contrast, the line Multipole 1 has an almost zero derivative at $Q^2 = 0$.

In the constant-cutoff approximation, we can also treat the cutoff $\Lambda_3 = \Lambda_4$ as an adjustable parameter, different from Λ_D, to be determined by a fit to the data. Different values of the cutoffs lead, however, to similar results. The combination of the form factors G_1 and G_2 on T_1 and T_2 is such that it generates an almost constant estimate for $A_{1/2}$, and an almost zero derivative for $A_{3/2}$ near $Q^2 = 0$.

The conclusion of this section is then that the data are not consistent with multipole parametrizations based on the same cutoff for G_1 and G_2.

C. Parametrization of G_i by multipole functions—natural scale

Since the universal cutoff fails to provide a description of the low-Q^2 transverse amplitude data, we look for alternative ways of defining the scale of variation of the elementary form factors G_i. Recalling that the nucleon elastic form factors and some inelastic transitions, such as the $\gamma^* N \to \Delta(1232)$ magnetic form factor, scale at sufficient small Q^2 with the dipole function (4.2), we wondered if the same scale can be used for the functions G_i. Since the functions are defined by different powers for the multipoles, the similarity of the functions G_i with G_D must be imposed for low Q^2. We consider then the conditions near $Q^2 = 0$,

$$\left(1+\frac{Q^2}{\Lambda_3^2}\right)^{-3} \simeq \left(1+\frac{Q^2}{\Lambda_D^2}\right)^{-2}, \quad (4.4)$$

[2]The term in Q^4 is very small because it is proportional to $1/(M_R+M)^4$.

$$\left(1+\frac{Q^2}{\Lambda_4^2}\right)^{-4} \simeq \left(1+\frac{Q^2}{\Lambda_D^2}\right)^{-2}. \tag{4.5}$$

The equivalence of the previous expansions near $Q^2 = 0$ implies that

$$\Lambda_3^2 = \frac{3}{2}\Lambda_D^2, \qquad \Lambda_4^2 = 2\Lambda_D^2. \tag{4.6}$$

Numerically, one has $\Lambda_3^2 \simeq 1.07$ GeV^2 and $\Lambda_4^2 \simeq 1.42$ GeV^2.

The numerical results associated with the multipole parametrization (4.1) with the cutoffs (4.6) and $G_3(0) = 0$ are presented in Figs. 1 and 2 by the thick solid line, and are labeled as Multipole 2a. Notice the closeness between the lines and the data.

Concerning the results from Fig. 2 for G_M, a note is in order. Since G_M depend only on G_1, all estimates discussed in this section have the same result for G_M (thick solid line). In the figure, we use the label Multipole 2.

The results of the parametrization Multipole 2a demonstrate that a reliable description of the $\gamma^* N \to N(1520)$ transverse amplitude data can be achieved when we assume the natural scale for the elementary form factors G_i.

We can now discuss the effect of the form factor G_3 in parametrizations of the data based on multipole functions. Although $G_3(0)$ cannot be determined by the $A_{1/2}(0)$ and $A_{3/2}(0)$ data, indirect information can be obtained from the amplitude $S_{1/2}$ at low Q^2. Unfortunately, no data below $Q^2 = 0.28$ GeV^2 are available to make a reliable estimate of $S_{1/2}(0)$, and consequently an estimate of $G_3(0)$.

In these conditions, one has to rely on theoretical extrapolations of the data. We consider then a parametrization of the data from Ref. [7], compatible with the pseudothreshold constraints of the helicity amplitudes, and also with the low-Q^2 data for $A_{1/2}$ and $A_{3/2}$. The value of $S_{1/2}(0)$ determined by that parametrization is $S_{1/2}(0) = -64.4 \times 10^{-3}$ GeV$^{-1/2}$. Combining this result with the present estimates of $G_1(0)$ and $G_2(0)$, one obtains $M^2 G_3(0) = -0.278$.

In addition to the parametrization discussed earlier [Multipole 2a, $G_3(0) = 0$], we consider also a parametrization with an intermediate value for $G_3(0)$, fixed by $M^2 G_3(0) = -0.14$, labeled as Multipole 2b, and a parametrization associated with value of $S_{1/2}(0)$ mentioned above (Multipole 2c). All parameters and associated values for $S_{1/2}(0)$ are presented in the last four rows of Table I.

The parametrizations labeled as Multipole 2b and Multipole 2c are also represented in Figs. 1 and 2 by the dashed lines (Multipole 2b) and the dashed-dotted lines (Multipole 2c).

Since these parametrizations (Multipoles 2a, 2b, 2c) are defined by the values of $G_1(0)$ and $G_2(0)$ determined by the transverse amplitudes at $Q^2 = 0$, one can also calculate the band of variation of the parametrizations based on the uncertainties of the parameters. For clarity, we include only the band of variation associated with the Multipole 2a. The others have similar ranges of variation from the central lines. The bands of variation are large for estimates near $Q^2 = 0$, when the errors are added in quadrature, mainly due to the large relative uncertainty of $A_{1/2}(0)$. For that reason, we restrict the representation to $Q^2 \geq 0.2$ GeV^2. The width of the bands decreases when Q^2 increases due to the reduction of the values of the functions G_i. More accurate experimental estimates of $A_{1/2}(0)$ and $A_{3/2}(0)$ will narrow the uncertainties of the estimates based on Eqs. (3.3), (3.4), (4.1), and (4.6).

From the analysis of the amplitudes (Fig. 1), we can conclude that the best description of the amplitude $A_{1/2}$ is obtained with Multipole 2a ($G_3 = 0$). Notice, however, that Multipole 2b provides also a fair description of the data when the uncertainties are taken into account. As for the amplitude $A_{3/2}$, Multipole 2b gives the best description when we consider the central values, but Multipole 2a and Multipole 2c are also consistent with the data when we take into account the uncertainties (upper error band for Multipole 2a and lower error band for Multipole 2c). Overall, Multipole 2a and Multipole 2b give the best combined description of the transverse amplitudes within the uncertainty bands. The agreement with the data is better for $Q^2 \leq 0.7$ GeV^2.

The preference for the parametrizations Multipole 2a and Multipole 2b favors also models with large magnitudes for the absolute values of the scalar amplitude $S_{1/2}(0)$, associated with the range $-(75...85) \times 10^{-3}$ GeV$^{-1/2}$, as indicated in Table I.

Similar conclusions are obtained when we look for the multipole form factors G_E and G_M (Fig. 2). All parametrizations are equivalent for G_M. The data for G_E favor the parametrizations Multipole 2a and Multipole 2b, within the intervals of variation.

In the graph for G_M, one can also observe that the function is very smooth near $Q^2 = 0$, contrasting with the sharp variation of G_E. This effect is a consequence of the particular condition for G_M at the pseudothreshold, as discussed in Sec. II A. No equivalent condition exists for G_E and G_C (related by $G_E \propto G_C$). Both functions, G_E and G_C, are finite at the pseudothreshold.

A consequence of the condition $G_M = 0$ at the pseudothreshold is that we can expect a turning point of the function below $Q^2 = 0.2$ GeV^2. The present calculations suggest that the turning point is close to $Q^2 = 0$, meaning that the derivative of G_M at photon point is close to zero. Considering the relation between G_M and G_1, we can conclude that $(M_R - M)^2 \frac{dG_M}{dQ^2}(0) = (1 - 3\frac{(M_R-M)^2}{\Lambda_3^2}) G_M(0) \simeq 0.05 G_M(0)$, consistent with a very small value for $\frac{dG_M}{dQ^2}(0)$. This result is a direct consequence of the parameter $\Lambda_3^2 = 1.07$ GeV^2.

The parametrizations discussed above can also be compared with recent parametrizations proposed in the literature. Of particular interest is the parametrization from Refs. [40,41] mentioned here as the JLab parametrization. The JLab parametrization is based on rational functions calibrated by JLab/CLAS and PDG ($Q^2 = 0$) data. The parametrization is close to the Multipole 2a parametrization within one standard deviation for $A_{3/2}$ and one or two standard deviations for $A_{1/2}$ in the $Q^2 < 0.8$ GeV^2 region (estimated by Multipole 2a). It provides also a good description of the large-Q^2 data.

The JLab parametrization has an important property: although the extension of the parametrization to the $Q^2 < 0$ region is not compatible with the pseudothreshold constraints, it can be analytically continued to the timelike region, in order to fulfill the pseudothreshold constraints [7]. This analytic continuation provides a soft transition between the region $Q^2 \simeq 0$ and the pseudothreshold and leaves the original parametrization of the region $0 \leq Q^2 \leq 0.8$ GeV^2 almost unchanged. Overall, one obtains a parametrization consistent with the low-Q^2 data and the necessary pseudothreshold constraints, preserving at the same time the original form for the large-Q^2 region [7].

D. Discussion

The parametrizations discussed above are based on two parameters, $G_1(0)$ and $G_2(0)$, a cutoff determined by theoretical arguments, and some tentative estimates of $G_3(0)$. Two of the parametrizations provide good descriptions of the data for $A_{1/2}$ and $A_{3/2}$ for $Q^2 < 1$ GeV^2, and determine also the possible range variation for the amplitude $S_{1/2}$ near $Q^2 = 0$.

From our analysis, we conclude also that the data favor parametrizations with multipole functions regulated by large cutoffs (Λ_3^2, $\Lambda_4^2 > 1$ GeV^2) and slower falloffs. The considered cutoffs are larger than the cutoff associated with the nucleon elastic form factors ($\Lambda_D^2 \simeq 0.7$ GeV^2).

In principle, more accurate estimates can be obtained considering extensions of the multipole parametrizations, where the second derivatives of G_i are adjusted by the low-Q^2 data. We did not test this possibility, because the main goal of the present work is the understanding of the $Q^2 = 0$ and low-Q^2 data based on a minimal number of parameters and assumptions.

The parametrizations proposed here may be tested in the near future by experiments in the range $Q^2 = 0 \ldots 0.3$ GeV^2, in order to fill the gap in the experimental studies of the $N(1520)$ resonance. Those data may be acquired at MAMI ($Q^2 > 0.2$ GeV^2) and JLab ($Q^2 > 0.05$ GeV^2) [4,10].

New data can help to determine the shape of the transverse amplitudes below $Q^2 = 0.3$ GeV^2, and impose more accurate constraints on parametrizations of the data near $Q^2 = 0$ [7]. The knowledge of the Q^2 dependence of the helicity amplitudes near $Q^2 = 0$ is important for the study of the $\gamma^* N \to N(1520)$ in the timelike region ($Q^2 < 0$), including the Dalitz decay of the $N(1520)$ state [$N(1520) \to e^+ e^- N$] [19,42].

V. OUTLOOK AND CONCLUSIONS

The $N(1520)$ resonance is among the nucleon excitations that are better known experimentally. It differs from the other low-lying nucleon resonances by its properties. The transverse amplitudes $A_{1/2}$ and $A_{3/2}$ have completely different magnitudes at $Q^2 = 0$, and are subject to relevant constraints at low Q^2, due to the proximity between the pseudothreshold $Q^2 = -(M_R - M)^2$ and the photon point.

In the present work, we looked for the origin of the difference of magnitudes between the transverse amplitudes at very low Q^2. We concluded that the result is related to a significant cancellation near $Q^2 = 0$ of the contributions associated with two elementary form factors (G_1 and G_2), defined by a gauge-invariant parametrization of the transition current. We concluded also that the correlation between the elementary form factors does not hold for larger values of Q^2.

To explain the shape of the amplitudes $A_{1/2}$ and $A_{3/2}$ below $Q^2 = 1$ GeV^2, in addition to the values of G_1 and G_2 at $Q^2 = 0$, one needs to know the scale of variation of the elementary form factors G_1, G_2, and G_3. We obtain a fair description of the $Q^2 \leq 0.7$ GeV^2 data when the scale of variation of the elementary form factors is correlated to the natural scale of the $\gamma^* N \to N^*$ transition amplitudes, defined by the nucleon dipole form factor.

Different parametrizations can be derived depending on the projected value of the scalar amplitude $S_{1/2}$ near $Q^2 = 0$. Those parametrizations are compatible with the experimental data for the transverse amplitudes within the uncertainties of the data for $Q^2 = 0$. The uncertainties can be reduced once the more accurate determinations of the transverse amplitudes are provided, mainly for $A_{1/2}(0)$. The proposed parametrizations explain also the smooth behavior of the magnetic dipole form factor G_M near $Q^2 = 0$, suggested by the data.

Our analysis of the transverse amplitudes $A_{1/2}$ and $A_{3/2}$ for finite Q^2 allows us to make an estimate of the range of variation of the scalar amplitude $S_{1/2}$ near $Q^2 = 0$, in a region for which there are no data available. Our parametrizations are compatible with values of $S_{1/2}(Q^2)$ in the range from -85×10^{-3} GeV$^{-1/2}$ to -75×10^{-3} GeV$^{-1/2}$, for values of Q^2 near the photon point. The parametrizations discussed in the present work may be tested in future measurements of the transverse and longitudinal amplitudes for $0 < Q^2 < 0.28$ GeV^2.

ACKNOWLEDGMENTS

G. R. was supported the Basic Science Research Program through the National Research Foundation of Korea (NRF) funded by the Ministry of Education (Grant No. NRF–2021R1A6A1A03043957).

[1] G. Ramalho and M. T. Peña, Prog. Part. Nucl. Phys. **136**, 104097 (2024).
[2] I. G. Aznauryan and V. D. Burkert, Prog. Part. Nucl. Phys. **67**, 1 (2012).
[3] I. G. Aznauryan *et al.*, Int. J. Mod. Phys. E **22**, 1330015 (2013).
[4] V. I. Mokeev, P. Achenbach, V. D. Burkert, D. S. Carman, R. W. Gothe, A. N. Hiller Blin, E. L. Isupov, K. Joo, K. Neupane, and A. Trivedi, Phys. Rev. C **108**, 025204 (2023).
[5] D. Drechsel, S. S. Kamalov, and L. Tiator, Eur. Phys. J. A **34**, 69 (2007).
[6] V. D. Burkert and T. S. H. Lee, Int. J. Mod. Phys. E **13**, 1035 (2004).
[7] G. Ramalho, Phys. Rev. D **100**, 114014 (2019).
[8] L. Tiator, Few-Body Syst. **57**, 1087 (2016).
[9] R. L. Workman *et al.* (Particle Data Group), Prog. Theor. Exp. Phys. **2022**, 083C01 (2022).
[10] V. I. Mokeev, and D. S. Carman (CLAS Collaboration), Few-Body Syst. **63**, 59 (2022).
[11] R. C. E. Devenish, T. S. Eisenschitz, and J. G. Korner, Phys. Rev. D **14**, 3063 (1976).
[12] G. Ramalho, Phys. Rev. D **93**, 113012 (2016).
[13] G. Ramalho, Phys. Rev. D **94**, 114001 (2016).
[14] G. Ramalho, Phys. Lett. B **759**, 126 (2016).
[15] Siegert's theorem is a general condition valid for the $\gamma^* N \to N^*$ transitions that relate the electric amplitude (combination of $A_{1/2}$ and $A_{3/2}$) and the scalar/longitudinal amplitude $S_{1/2}$ near $Q^2 = -(M_R - M)^2$.
[16] D. Drechsel and L. Tiator, J. Phys. G **18**, 449 (1992).
[17] A. J. Buchmann, E. Hernandez, U. Meyer, and A. Faessler, Phys. Rev. C **58**, 2478 (1998).
[18] M. Warns, W. Pfeil, and H. Rollnik, Phys. Rev. D **42**, 2215 (1990).
[19] G. Ramalho and M. T. Peña, Phys. Rev. D **89**, 094016 (2014); **95**, 014003 (2017).
[20] V. I. Mokeev, V. D. Burkert, D. S. Carman, L. Elouadrhiri, G. V. Fedotov, E. N. Golovatch, R. W. Gothe, K. Hicks, B. S. Ishkhanov, E. L. Isupov *et al.*, Phys. Rev. C **93**, 025206 (2016).
[21] D. Merten, R. Ricken, M. Koll, B. Metsch, and H. Petry, Eur. Phys. J. A **13**, 477 (2002).
[22] M. Ronniger and B. C. Metsch, Eur. Phys. J. A **49**, 8 (2013).
[23] M. M. Giannini and E. Santopinto, Chin. J. Phys. **53**, 020301 (2015).
[24] B. Golli and S. Širca, Eur. Phys. J. A **49**, 111 (2013).
[25] R. Bijker and E. Santopinto, Phys. Rev. C **80**, 065210 (2009).
[26] B. Julia-Diaz, T. S. H. Lee, A. Matsuyama, T. Sato, and L. C. Smith, Phys. Rev. C **77**, 045205 (2008).
[27] H. Kamano, S. X. Nakamura, T. S. H. Lee, and T. Sato, Phys. Rev. C **88**, 035209 (2013).
[28] G. Ramalho, Phys. Rev. D **95**, 054008 (2017).
[29] H. F. Jones and M. D. Scadron, Ann. Phys. (N.Y.) **81**, 1 (1973).
[30] T. De Forest, Jr. and J. D. Walecka, Adv. Phys. **15**, 1 (1966).
[31] E. Amaldi, S. Fubini, and G. Furlan, Springer Tracts Mod. Phys. **83**, 1 (1979).
[32] G. Ramalho, Eur. Phys. J. A **54**, 75 (2018).
[33] C. E. Carlson, Phys. Rev. D **34**, 2704 (1986); C. E. Carlson and J. L. Poor, Phys. Rev. D **38**, 2758 (1988).
[34] C. E. Carlson and N. C. Mukhopadhyay, Phys. Rev. D **58**, 094029 (1998).
[35] I. G. Aznauryan *et al.* (CLAS Collaboration), Phys. Rev. C **80**, 055203 (2009).
[36] V. I. Mokeev *et al.* (CLAS Collaboration), Phys. Rev. C **86**, 035203 (2012).
[37] V. D. Burkert, R. De Vita, M. Battaglieri, M. Ripani, and V. Mokeev, Phys. Rev. C **67**, 035204 (2003).
[38] V. Pascalutsa and M. Vanderhaeghen, Phys. Rev. D **73**, 034003 (2006).
[39] G. Eichmann and G. Ramalho, Phys. Rev. D **98**, 093007 (2018).
[40] A. N. Hiller Blin, V. Mokeev, M. Albaladejo, C. Fernández-Ramírez, V. Mathieu, A. Pilloni, A. Szczepaniak, V. D. Burkert, V. V. Chesnokov, A. A. Golubenko *et al.*, Phys. Rev. C **100**, 035201 (2019).
[41] https://userweb.jlab.org/~isupov/couplings.
[42] R. Abou Yassine *et al.* (HADES Collaboration), arXiv: 2205.15914; arXiv:2309.13357.